

---

# Effect of Acid Treatment on the Structure of Natural Zeolite from the Shankanay Deposit

---

[Tanirbergenova Kudaibergenova Sandugash](#)\*, [D.A. Tugelbayeva](#), [N.K Zhylybayeva](#), [Aitugan Aizat](#)\*,  
Tazhu Kairat, [Moldazhanova G.M.](#), [Mansurov Z.M.](#)

Posted Date: 11 August 2025

doi: 10.20944/preprints202505.2097.v2

Keywords: natural zeolite; modified zeolite; clinoptilolite; acid activation; mixed acid treatment; surface area; microporosity; hydrodesulfurization (HDS); thiophene removal; catalyst support; shankhanai deposit



Preprints.org is a free multidisciplinary platform providing preprint service that is dedicated to making early versions of research outputs permanently available and citable. Preprints posted at Preprints.org appear in Web of Science, Crossref, Google Scholar, Scilit, Europe PMC.

Copyright: This open access article is published under a Creative Commons CC BY 4.0 license, which permit the free download, distribution, and reuse, provided that the author and preprint are cited in any reuse.

*Article*

# Effect of Acid Treatment on the Structure of Natural Zeolite from the Shankanay Deposit

Tanirbergenova Kudaibergenova Sandugash \*, D. A. Tugelbayeva, N. K. Zhylybayeva, Aitugan A. N. \*, Tazhu K., Moldazhanova G. M. and Mansurov Z. A.

The Institute of Combustion Problems, Almaty, Kazakhstan

\* Correspondence: sandu2201@mail.ru (T.K.S.); aizataitugan@gmail.com (A.A.N.)

## Abstract

Natural clinoptilolite from the Shankhanai deposit (Kazakhstan) was modified via acid and thermal treatments to improve its physicochemical and catalytic properties. The zeolite was activated using 10% nitric acid alone, nitric acid followed by thermal treatment (600 °C), and a mixed acid solution (10% HNO<sub>3</sub> + 5% CH<sub>3</sub>COOH) followed by mild thermal treatment (280 °C). Structural, textural, and thermal changes were characterized by XRD, FTIR, BET, TGA, SEM, and EDX. While nitric acid improved surface area (BET up to 59.9 m<sup>2</sup>/g), it compromised crystallinity. The mixed acid approach effectively enhanced porosity and acidity while preserving structural integrity. Preliminary catalytic testing in thiophene hydrodesulfurization showed improved conversion (up to 20.7%) in the absence of active metals, confirming the potential of modified zeolite as a catalyst support. The dual-acid method presents a promising, eco-friendly pathway for producing thermally stable and catalytically active zeolitic materials.

**Keywords:** natural zeolite; modified zeolite; clinoptilolite; acid activation; mixed acid treatment; surface area; microporosity; hydrodesulfurization (HDS); thiophene removal; catalyst support; shankhanai deposit

## 1. Introduction

Sulfur-containing compounds in petroleum fractions, such as thiophene and its derivatives, present significant environmental and technological challenges. Upon combustion, they form sulfur oxides (SO<sub>x</sub>), which contribute to acid rain and air pollution. Additionally, sulfur deactivates catalysts in downstream refining and deteriorates fuel quality. Therefore, the development of efficient hydrodesulfurization (HDS) technologies remains a priority in petroleum refining, driven by stringent international regulations, including the EU Directive 2009/30/EC (≤10 ppm sulfur in fuels) and IMO 2020 (≤0.5% sulfur in marine fuels) [1,2]. Among sulfur heterocycles, thiophene is particularly resistant to conventional HDS due to its chemical stability, necessitating advanced catalytic systems capable of operating under mild conditions. Catalyst supports play a critical role in such systems by affecting the dispersion, stability, and activity of the active phase. Various materials have been explored as HDS supports, including  $\gamma$ -Al<sub>2</sub>O<sub>3</sub>, SiO<sub>2</sub>, TiO<sub>2</sub>, and activated carbons [3–8]. Recently, natural zeolites have gained increasing attention owing to their unique structural and surface properties—high surface area, tunable acidity, ion-exchange capacity, and thermal stability. In contrast to synthetic materials, they are also cost-effective and readily available, especially in regions with natural deposits.

Zeolites are natural or synthetic crystalline aluminosilicates with a microporous structure. Their framework consists of TO<sub>4</sub> tetrahedra (where T = Si or Al) linked into a three-dimensional network. These materials possess ion-exchange, adsorption, and catalytic properties. They also exhibit high thermal and chemical stability. These characteristics make zeolites promising for use in petrochemistry, environmental engineering, and clean fuel production [1–4,9–12]. One of the main natural zeolite deposits in Central Asia is the Shankhanai deposit, located in the Kerbulak district of

Almaty region, Kazakhstan. Its reserves are estimated at 4.3 million tons. The dominant zeolite phase in this deposit is heulandite–clinoptilolite. It has a monoclinic structure ( $a = 17.64 \text{ \AA}$ ;  $b = 17.88 \text{ \AA}$ ;  $c = 7.40 \text{ \AA}$ ;  $\beta = 116.30^\circ$ ) and the chemical formula  $[\text{KNa}_2\text{Ca}_2(\text{Si}_{29}\text{Al}_7)\text{O}_{72}\cdot 32\text{H}_2\text{O}]$ . The main difference between heulandite and clinoptilolite is the Si/Al ratio. For heulandite, it is around 2.9–3.0, while for clinoptilolite, it is 5.0 or higher [13,14].

Clinoptilolite is the main zeolite in this deposit. It is an aluminosilicate matrix with well-developed microporosity. It can selectively adsorb molecules and participate in ion exchange. Its natural analogs, such as faujasite, mordenite, and synthetic HZSM-5, are widely used as catalysts. These catalysts are applied in cracking, isomerization, alkylation, alcohol dehydration, and hydrocracking of hydrocarbons [15–18]. However, natural zeolites, including clinoptilolite, have limited catalytic activity. This is due to their relatively low acidity and small pore size. Acid modification can improve their catalytic performance. During acid treatment, aluminum is partially removed from the framework (dealumination). This process increases the Si/Al ratio, exposes active sites, and enhances porosity and surface area [19–21]. At the same time, the zeolite framework remains intact, which is important for stability [22].

Acid treatment is a simple and scalable method to improve the textural and catalytic properties of zeolites. It promotes the formation of mesopores and macropores. This improves diffusion and access to active sites [19]. Acid treatment also increases surface acidity. This includes the formation of Brønsted and Lewis acid sites, confirmed by pyridine-FTIR and  $\text{NH}_3$ -TPD methods [20]. Zeolites from the Shankhanai deposit are of special interest. They contain eight-membered rings and have a high Si/Al ratio. These features provide thermal stability and surface acidity. To enhance the sorption and catalytic properties of natural zeolites, acid activation is commonly used. This method removes exchangeable cations ( $\text{Na}^+$ ,  $\text{K}^+$ ,  $\text{Ca}^{2+}$ ) and partially leaches aluminum from the framework. As a result, acid sites are formed and porosity is increased [21]. A comparative analysis of different acids shows that hydrochloric acid (HCl) effectively removes cations and causes partial desilication. This increases surface area. However, at high concentrations, HCl may lead to partial amorphization of the zeolite structure [22,23]. Sulfuric acid ( $\text{H}_2\text{SO}_4$ ) can cause the precipitation of sulfates. These precipitates may block pores and reduce access to active sites. Acetic acid ( $\text{CH}_3\text{COOH}$ ) is a weak organic acid. It allows gentle modification without destroying the structure. However, it does not significantly increase acidity or porosity. In contrast, nitric acid ( $\text{HNO}_3$ ) has strong oxidizing and protolytic properties. It effectively removes cations and promotes the formation of both Brønsted and Lewis acid sites [24,25].

Clinoptilolite from the Shankhanai deposit has high thermal stability. It maintains its structure up to  $\sim 500 \text{ }^\circ\text{C}$ . It also shows good mechanical strength and acid resistance in granulated form. These properties make it suitable for use in gas purification and low-carbon technologies. Due to its ion-exchange structure, it can selectively adsorb molecules based on size (molecular sieve effect). It is resistant to catalyst poisons and can be regenerated during use. This makes it a low-cost and accessible natural catalyst for eco-friendly hydrocarbon processing [26,27]. Thermal post-treatment was used to increase the stability and porosity of the acid-treated zeolite. This step removed residual moisture and improved structural order, preventing further degradation of the framework. The use of argon ensures the absence of oxidative processes during heating. Such thermal stabilization is known to promote the development of mesoporosity and improve the availability of active sites in modified clinoptilolite [28]. Zeolites from the Shankhanai deposit are of particular interest. Their eight-membered rings and high Si/Al ratio provide thermal stability and surface acidity [29,30]. However, natural zeolites of this type in Kazakhstan remain poorly studied. This includes their acid modification and changes in microporosity and acidity [31–33].

This study focuses on a natural zeolite from the Shankanay deposit, Kazakhstan, which represents a locally sourced, abundant, and underutilized resource. The goal is to evaluate the effect of acid treatment on the crystalline structure, textural, and acidic properties. The following techniques were used: FTIR, XRD, SEM, BET,  $\text{NH}_3$ -TPD, and pyridine-FTIR. This analysis helps identify new aspects of zeolite activity as a catalyst support for thiophene hydrodesulfurization and demonstrates the scientific novelty of the research.

## 2. Materials and Methods

### 2.1. Acid Activation of Natural Zeolite

Natural zeolite (clinoptilolite) from the Shankhanai deposit (Almaty Region, Kazakhstan) was subjected to acid activation using two different treatments. In the first case, 400 g of the ground zeolite was treated with a 10% nitric acid (HNO<sub>3</sub>) (chemically pure, GOST 4461-77, manufacturer JSC Lenreaktiv) solution; in the second 10% nitric acid (HNO<sub>3</sub>) and thermal treatment, in third a mixed solution of 10% HNO<sub>3</sub> and 5% acetic acid (CH<sub>3</sub>COOH) (acetic acid, 70%, manufacturer JSC Base of Chemical Reactants) was used. The acid treatments were performed in round-bottom flasks equipped with reflux condensers under continuous magnetic stirring at the respective boiling temperatures of the acids for 24 hours.

After the reaction, the zeolite suspension was cooled and filtered. The solid phase was washed multiple times with deionized water until a neutral pH (6–7) was reached, measured using a calibrated pH meter (ITAN, LLC "NPP Tomanalit", Russian Federation). The washed zeolite was then dried at 120 °C for 1 hour in a convection oven.

### 2.2. Thermal Treatment of Activated Zeolite

Thermal treatment was performed after acid activation to enable further investigation of structural modifications. The zeolite activated with 10% nitric acid was subjected to thermal treatment at 600 °C for 1 hour in an argon atmosphere (inert gas environment) using a tubular furnace (manufacturer: Nabertherm, Germany). In the second case, the zeolite activated with a mixed solution of 10% nitric acid (HNO<sub>3</sub>) and 5% acetic acid (CH<sub>3</sub>COOH) was thermally treated at 280 °C for 15 minutes in an argon atmosphere. The heating rate in both cases was controlled at 10 °C/min. After thermal treatment, the samples were allowed to cool to room temperature under argon flow and stored in sealed containers for further analysis. The zeolite samples were then labeled as follow: Natural Zeolite (NZ), 10% nitric acid (HNO<sub>3</sub>) treated zeolite (Z- HNO<sub>3</sub>), 10% nitric acid (HNO<sub>3</sub>) and thermal treatment (Z- HNO<sub>3</sub>-600), treated with mix solution of 10% HNO<sub>3</sub> and 5% acetic acid (CH<sub>3</sub>COOH) zeolite (Z-MIX-280).

### 2.3. Characterization Techniques

Fourier Transform Infrared Spectroscopy (FTIR): Infrared spectra were recorded using a Bruker ALPHA II FTIR spectrometer in the range of 500–3500 cm<sup>-1</sup>. The samples were prepared by the standard KBr pellet method: approximately 1 mg of finely ground zeolite sample was thoroughly mixed with 200 mg of dry KBr and pressed into a transparent pellet under vacuum. The characteristic absorption bands were analyzed to monitor structural changes in the zeolite framework.

X-ray Diffraction (XRD): X-ray diffraction patterns were obtained using a DW-XRD-27MINI diffractometer with CuK $\alpha$  radiation ( $\lambda = 1.5418 \text{ \AA}$ ), operating in Bragg–Brentano ( $\theta$ – $2\theta$ ) geometry. The current and voltage of the X-ray tube were set at 30 mA and 40 kV, respectively. Samples were ground, pressed into holders, and measured with continuous rotation at 60 rpm.

Elemental composition and surface morphology of the zeolite samples were examined using a Phenom ProX SEM (Thermo Fisher Scientific, USA) equipped with an EDX detector. Samples were prepared by both dry powder and suspension mounting on carbon tape. Measurements were conducted under vacuum in backscattered electron mode.

Nitrogen adsorption–desorption isotherms were obtained using a **BSD-660S A3 Physical Adsorption Analyzer** (BSD INSTRUMENT, China) at 77.3 K, employing high-purity nitrogen as the adsorbate. Prior to measurements, samples were degassed in situ under vacuum at 300 °C for 180 min to eliminate moisture and volatile impurities. The specific surface area was calculated using the Brunauer–Emmett–Teller (BET) method within the relative pressure ( $P/P_0$ ) range of 0.03–0.25. Pore volume and pore size distribution were derived from the desorption branch using the Barrett–Joyner–Halenda (BJH) method. Micropore characteristics were additionally analyzed using the

Dubinin–Radushkevich (DR), Dubinin–Astakhov (DA), and t-plot methods. All measurements and data processing were carried out using the instrument's proprietary analysis software.

Thermal behavior and stability of the natural and acid-treated zeolite samples were analyzed using a TGA/DSC instrument (Mettler Toledo, Switzerland). Approximately 10–15 mg of each powdered sample was placed in an open alumina crucible and subjected to heating from room temperature to 900 °C at a constant heating rate of 10 °C/min under a nitrogen atmosphere (flow rate ~50 mL/min). The TGA curves were used to evaluate mass loss associated with the desorption of physically adsorbed water, removal of surface groups, and potential framework degradation. Simultaneously recorded DSC curves provided insights into endothermic and exothermic events related to structural transformations and decomposition processes.

#### 2.4. Catalytic Activity

The catalytic activity of natural zeolite was tested in thiophene hydrodesulfurization in a n-heptane stream as a model reaction in the fixed-bed stainless steel reactor under hydrogen flow at 180–380 °C and 0.1–3.0 MPa. The modified zeolite (14 mL, particle size 0.63–1 mm) was pre-reduced in hydrogen and then contacted with a model feedstock. The system included a condenser and two-stage gas–liquid separation for product collection. Reaction products were analyzed by gas chromatography to evaluate sulfur removal efficiency.

### 3. Results

#### 3.1. Physicochemical Characterization of Zeolite (Clinoptilolite) from the Shankhanai Deposit

A comprehensive physicochemical characterization of the natural and acid-treated zeolite samples was conducted to investigate the influence of acid treatment on their structural, textural, thermal, and morphological properties. The characterization techniques included X-ray diffraction (XRD), Fourier-transform infrared spectroscopy (FTIR), nitrogen adsorption–desorption isotherms (BET), thermogravimetric analysis (TGA), scanning electron microscopy (SEM), and energy-dispersive X-ray spectroscopy (EDX). The following sections summarize the results of each technique.

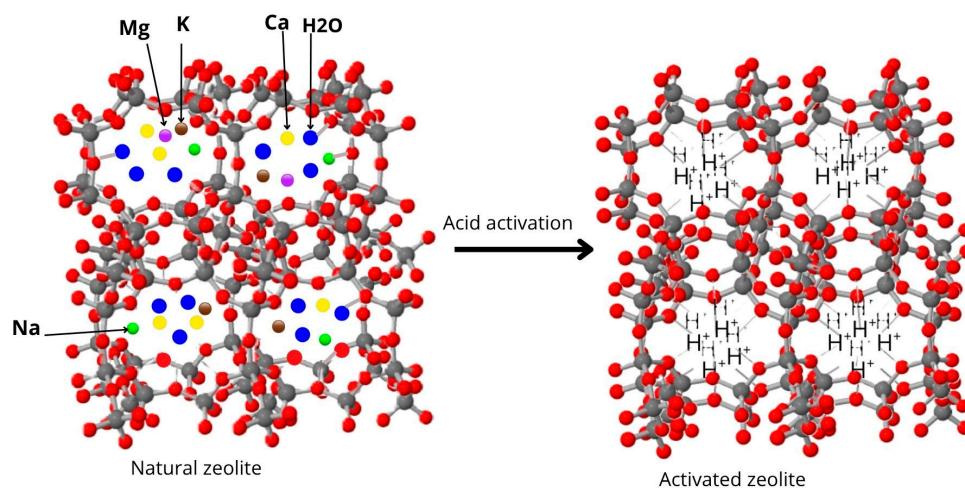


**Figure 1.** Schematic illustration of the structural modifications occurring in natural zeolite upon acid activation.

### 3.1.1. X-ray Diffraction (XRD)

The XRD patterns of the natural and acid-modified zeolite samples revealed significant differences in crystallinity. The XRD pattern of the natural zeolite (Figure 2a), confirms clinoptilolite as the dominant crystalline phase, with sharp peaks between  $19^\circ$  and  $50^\circ$   $2\theta$ . The most intense reflection at  $2\theta = 26.59^\circ$  corresponds to the (040) plane, indicating high crystallinity and preferred orientation. Additional peaks at  $2\theta = 19.70^\circ, 21.96^\circ, 23.55^\circ, 24.11^\circ, 27.90^\circ,$  and  $29.82^\circ$  match (020), (111), (200), (021), (240), and (151) planes, respectively, in agreement with JCPDS PDF #39-1383. Minor peaks suggest the presence of non-zeolitic phases. Semi-quantitative analysis indicates albite (35.8%), quartz (23.9%), potassium feldspar (19.1%), iron-rich silicate (15.6%), and hematite (5.6%), confirming a feldspar- and quartz-containing natural tuff matrix. After treatment with 10% nitric acid (Figure 2b), the XRD pattern shows structural transformation, with heulandite emerging as the main phase. The most intense peak at  $2\theta = 26.63^\circ$  corresponds to the (040) plane, with additional reflections (200), (131), (400), (151), and (062) at  $2\theta = 23.60^\circ, 25.98^\circ, 27.75^\circ, 29.89^\circ,$  and  $33.15^\circ$ . Broadened peaks at low angles ( $9.79^\circ, 11.18^\circ, 12.98^\circ$ ) and a weak amorphous halo indicate partial dealumination and framework degradation. Phase analysis reveals heulandite (43%), quartz (20%), albite (14%), boron-containing impurity (16%), and hematite (6%). While nitric acid enhances surface acidity by removing non-zeolitic phases, its aggressive action compromises crystallinity. Therefore, a milder activation strategy is considered.

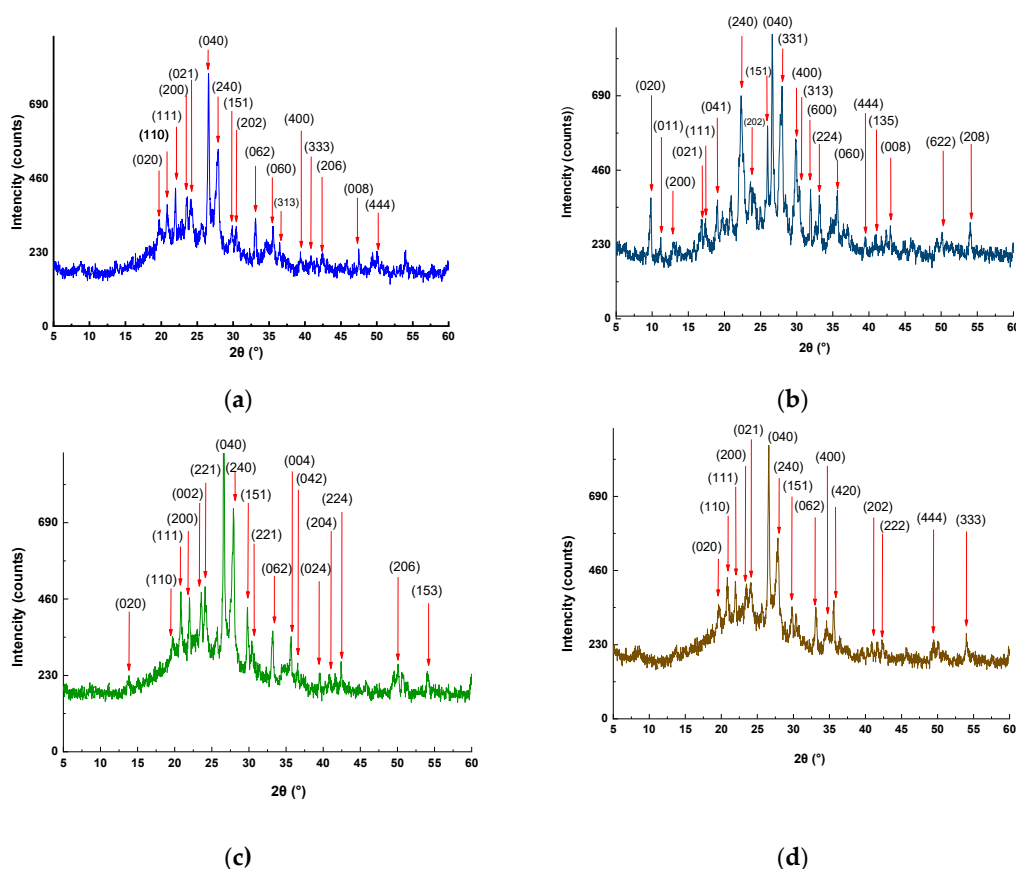


**Figure 2.** X-ray Diffractograms of the Natural and Modified Zeolite Samples Treated with Acids: (a) – NZ; (b) – Z- HNO<sub>3</sub>; (c) – Z- HNO<sub>3</sub>-600; (d) –Z-MIX-280.

The XRD pattern of the zeolite sample treated with 10% nitric acid and subsequently thermally activated at 600 °C (Figure 2c), in argon reveals enhanced crystallinity compared to the sample treated with acid alone. The most intense peak at  $2\theta = 26.62^\circ$  corresponds to the (040) plane of the

clinoptilolite–heulandite group, with additional reflections at  $23.57^\circ$ ,  $24.10^\circ$ ,  $27.91^\circ$ ,  $29.81^\circ$ , and  $33.17^\circ$ . Sharper peaks and a reduced amorphous background suggest improved structural order. Broader low-angle reflections ( $13.86^\circ$ ,  $19.72^\circ$ ) indicate partial dealumination with residual channel ordering. The thermal treatment was applied after acid activation, primarily to remove residual water and open the microporous network of the zeolite, aiding in the development of accessible acid sites. Semi-quantitative analysis indicates a composition dominated by albite (53%), potassium feldspar (23%), iron-rich silicate (11%), quartz (9%), and hematite (4%). Despite some framework modification, the crystalline phases remain well-defined, confirming that thermal post-treatment acts as a stabilizing step, enhancing porosity and structural retention following acid exposure. Combined treatment with 10% nitric acid and 5% acetic acid, followed by mild thermal activation at  $280^\circ\text{C}$  for 15 min (Figure 2d), preserves the clinoptilolite framework. The strongest peak at  $2\theta = 26.57^\circ$  (040 plane) and other reflections at  $19.77^\circ$ ,  $21.97^\circ$ ,  $23.50^\circ$ ,  $24.09^\circ$ ,  $27.85^\circ$ ,  $29.81^\circ$ , and  $33.12^\circ$  correspond to typical clinoptilolite planes, with no amorphous background. The gentler acid environment, due to acetic acid buffering, minimizes dealumination while enhancing acidity. Phase composition indicates albite (53%), K-feldspar (23%), iron-rich silicate (11%), quartz (9%), and hematite (4%). This dual-acid, low-temperature strategy maintains crystallinity while introducing acid sites, making it suitable for catalytic applications.

In summary, XRD analysis demonstrates that acid and thermal treatments significantly influence the phase composition and crystallinity of natural clinoptilolite-based zeolite. Strong acid treatment with  $\text{HNO}_3$  leads to partial framework degradation and phase transformation toward heulandite, while thermal post-treatment helps restore order and stabilize the structure. The combined use of nitric and acetic acids, followed by mild thermal activation, effectively preserves the clinoptilolite framework, indicating a balanced approach to modifying acidity without compromising crystallinity. Following the structural insights obtained from XRD analysis, which highlighted changes in crystallinity and phase composition upon acid and thermal treatments, further investigation was conducted using Fourier-transform infrared (FTIR) spectroscopy.

### 3.1.2. FTIR Analysis

FTIR spectra of the Natural and Modified Zeolite Samples Treated with Acids within the  $500\text{--}3000\text{ cm}^{-1}$  range in the Figure 3. Characteristic bands are observed at  $\sim 1030\text{ cm}^{-1}$  and  $799\text{--}787\text{ cm}^{-1}$ , corresponding to the asymmetric stretching vibrations of Si–O–Si and/or Si–O–Al linkages and the symmetric stretching of internal tetrahedral units, respectively in the FTIR spectrum of the natural zeolite (Figure 3a). The bands in the  $600\text{--}650\text{ cm}^{-1}$  region ( $645$ ,  $633$ ,  $616\text{ cm}^{-1}$ ) are attributed to framework bending vibrations, typical for clinoptilolite zeolites.

Upon treatment with nitric acid, new bands appear at  $\sim 2363$  and  $2332\text{ cm}^{-1}$  (Figure 3b), which can be assigned to adsorbed  $\text{CO}_2$  or nitrate species trapped in the porous structure. A notable band at  $1649\text{ cm}^{-1}$  is associated with the bending vibration of water molecules, indicating increased hydrophilicity due to dealumination and the formation of new Brønsted acid sites. Slight shifts in the Si–O–T (T = Si, Al) vibrations suggest partial framework disturbance. These spectral changes suggest alterations in the short-range ordering of the zeolite framework, possibly due to dealumination or framework disruption upon acid and thermal treatment, as also confirmed by XRD. Further thermal treatment ( $280^\circ\text{C}$ ) of the nitric acid-modified zeolite leads to additional changes. The bands at  $1706$ ,  $1541$ , and  $1501\text{ cm}^{-1}$  may be related to the presence of carboxylate or residual nitrate species undergoing decomposition (Figure 3c).

The reduction in intensity of the  $1644\text{ cm}^{-1}$  band and the emergence of sharper signals near  $1032\text{ cm}^{-1}$  indicate removal of physisorbed water and improved stabilization of acid-modified sites. Thermal activation at this stage aids in cleaning the pore structure and enhances thermal resistance, making the material more suitable for catalytic applications. The zeolite treated with a mixture of acetic and nitric acids followed by thermal treatment exhibits features of both acid modification and thermal stabilization. The presence of intense bands at  $1719$ ,  $1561$ , and  $1505\text{ cm}^{-1}$  is indicative of new surface functionalities, possibly linked to acetate interactions or enhanced Brønsted/Lewis acidity.

Importantly, the Si–O–T stretching band at  $1032\text{ cm}^{-1}$  remains strong and well-defined, indicating preservation of the zeolite framework (Figure 3d). Compared to nitric acid treatment alone, this dual acid treatment enables a higher density of acidic sites while maintaining the integrity of the microporous structure. Thermal activation promotes the removal of moisture and organics, ensuring stability under catalytic conditions.

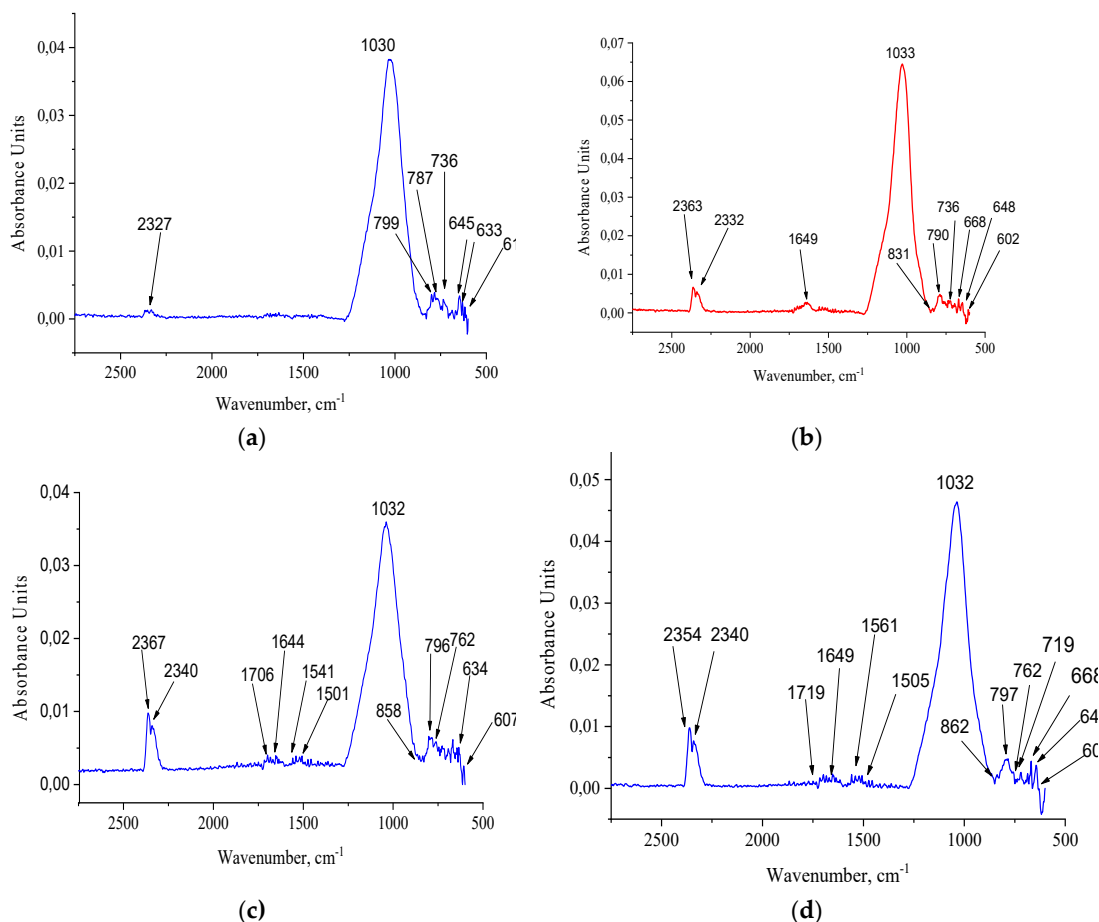


**Figure 3.** FTIR Spectra of the Natural and Modified Zeolite Samples Treated with Acids: (a) – NZ; (b) – Z-  $\text{HNO}_3$ ; (c) – Z-  $\text{HNO}_3$ -600; (d) – Z-MIX-280.

Overall, the FTIR results confirm that nitric acid increases surface acidity but may compromise structural stability, while subsequent thermal treatment and mixed acid approaches improve acid site density and preserve the structural framework—key properties for catalytically active zeolites.

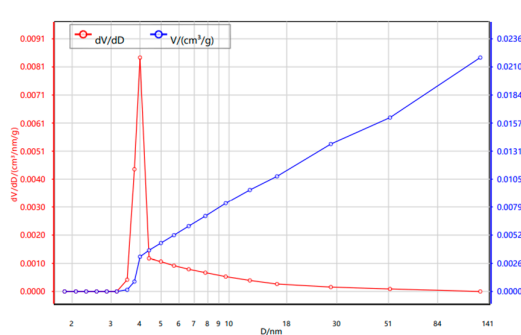
### 3.1.3. $\text{N}_2$ Adsorption–Desorption Isotherms (BET)

The textural properties of the natural and modified zeolite samples were investigated using nitrogen adsorption–desorption at 77 K. The isotherms and corresponding BET data are shown in Figure 4 and Table 1.

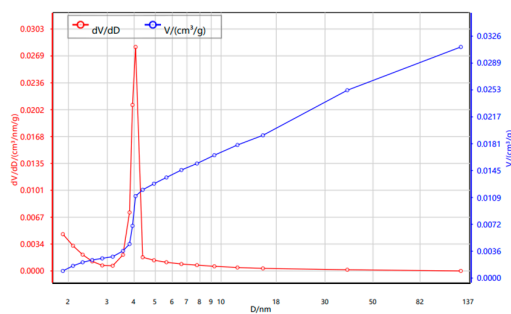
**Table 1.** Textural properties of the natural and modified zeolite samples.

Sample	BET SSA (m <sup>2</sup> /g)	DR Micropore SSA (m <sup>2</sup> /g)	DA Micropore Volume (cm <sup>3</sup> /g)	DR Avg. Pore Diameter (nm)	Average Pore Diameter (4V/A, nm)
NZ	4.95	5.91	0.0054	2.09	15.99
Z- HNO <sub>3</sub>	59.86	67.98	0.0330	1.36	3.26
Z- HNO <sub>3</sub> -600	19.39	21.09	0.0151	1.75	6.21
Z-MIX-280	48.07	54.50	0.0276	1.52	3.84

The BET and DR/DA analysis results (Table 1) clearly demonstrate the influence of acid activation and subsequent thermal treatment on the textural properties of the zeolite samples. The natural zeolite (NZ) exhibited a low specific surface area (BET: 4.95 m<sup>2</sup>/g), minimal micropore volume (0.0054 cm<sup>3</sup>/g), and a relatively large average pore diameter (~16 nm), which is typical for untreated clinoptilolite with blocked or partially collapsed micropores. Upon treatment with 10% nitric acid (Z-HNO<sub>3</sub>), a significant increase in specific surface area (up to 59.86 m<sup>2</sup>/g BET; 67.98 m<sup>2</sup>/g DR) and micropore volume (0.0330 cm<sup>3</sup>/g) was observed, accompanied by a decrease in average pore diameter (to ~3.26 nm). These changes reflect efficient dealumination, removal of exchangeable cations (Na<sup>+</sup>, K<sup>+</sup>, Ca<sup>2+</sup>), and partial unblocking or formation of new micropores, enhancing the adsorption capacity and acid site accessibility. The sample subjected to thermal treatment at 600 °C after nitric acid activation (Z-HNO<sub>3</sub>-600) exhibited a moderate decrease in surface area (BET: 19.39 m<sup>2</sup>/g), but retained improved porosity compared to the natural zeolite. The partial collapse of some newly formed micropores at elevated temperatures is likely compensated by the stabilization of remaining structural features. The increased average pore diameter (6.21 nm) indicates structural rearrangement and possible mesopore formation. In contrast, the sample treated with a mixture of 10% nitric acid and 5% acetic acid followed by thermal activation at 280 °C (Z-MIX-280) demonstrated a favorable balance between surface area (BET: 48.07 m<sup>2</sup>/g), micropore volume (0.0276 cm<sup>3</sup>/g), and pore size distribution. The combination of oxidizing (HNO<sub>3</sub>) and mild organic (CH<sub>3</sub>COOH) acids provided both surface activation and framework preservation, preventing excessive dealumination or collapse. As a result, the material maintained enhanced microporosity and moderate pore size (3.84 nm), optimal for catalytic applications requiring both accessibility and structural stability.



(a)



(b)

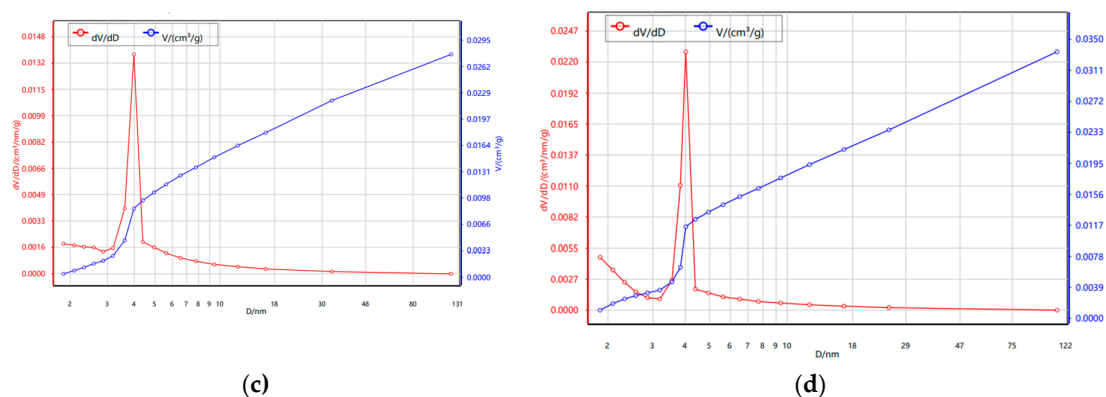


**Figure 4.** BJH(Desorption) Pore Volume & Pore Size Curve of the Natural and Modified Zeolite Samples Treated with Acids: (a) – NZ; (b) – Z- HNO<sub>3</sub>; (c) – Z- HNO<sub>3</sub>-600; (d) –Z-MIX-280.

The natural zeolite exhibits a relatively low pore volume with a broad distribution in the mesopore region (3–15 nm). HNO<sub>3</sub>-treated samples show a shift toward narrower mesopores (~3.5–5 nm) and significantly increased pore volume, indicating acid-induced framework opening. Thermal treatment after HNO<sub>3</sub> activation (Z-HNO<sub>3</sub>-600) results in slight pore shrinkage and structural reordering. In contrast, the dual-acid-treated sample (Z-MIX-280) demonstrates the highest pore volume and sharper mesopore distribution, suggesting enhanced pore accessibility and surface development. These findings highlight the role of acid and thermal treatments in tailoring zeolite porosity for catalytic applications.

Overall, the N<sub>2</sub> sorption data show that acid treatment with a mixture of nitric and acetic acid, especially when combined with thermal activation, significantly improves the textural characteristics of clinoptilolite, increasing its specific surface area and improving access to active sites - properties favourable for adsorption and catalytic applications.

### 3.1.4. Thermogravimetric Analysis (TGA)

The thermogravimetric analysis (TGA) of the natural clinoptilolite sample (NZ) demonstrates a nearly linear mass loss in the initial heating stage, with a slight decrease up to ~265 °C (Figure 5a). This weight reduction is primarily associated with the desorption of physically adsorbed water and loosely bound hydroxyl groups from the zeolitic framework. A subsequent plateau in the TGA curve (~270–660 °C) suggests temporary thermal stability of the natural zeolite, with no significant decomposition or structural disruption in this temperature range. A more pronounced mass loss occurs at ~670–700 °C, likely due to partial dehydroxylation or the release of strongly retained water or cation-associated species. Overall, the natural zeolite retains structural integrity up to at least 800 °C, confirming its high thermal stability. The acid-treated zeolite (Z-MIX-280) exhibits thermal behavior indicative of surface and structural modifications (Figure 5b). The first observable weight change occurs at ~353.5 °C, corresponding to the decomposition of surface functionalities introduced by acid treatment. A second mass loss at ~441.2 °C is likely due to the removal of nitrate or acetate residues trapped within micropores. Further inflection points at ~541.1 °C, ~647.5 °C, and ~816.7 °C suggest progressive breakdown or rearrangement of the modified framework. The cumulative weight loss reaches approximately 4% by the end of the analysis, with the residual mass stabilizing around 96%. Despite these changes, the acid-activated zeolite maintains thermal robustness, indicating that the treatment does not cause drastic degradation of the structure.



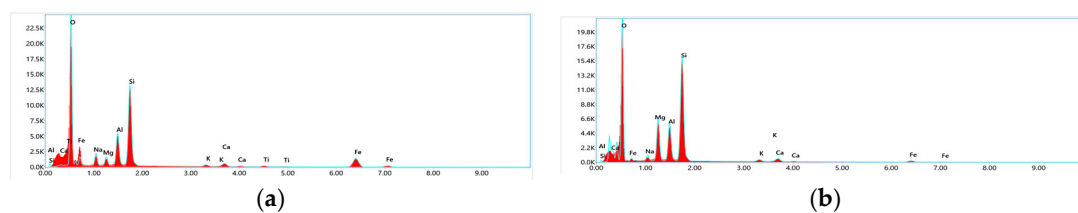
The particles remain in the medium size range (approximately 14–44.7  $\mu\text{m}$ ) (Figure 6b), but the regular distribution of pores is disrupted, and the overall framework shows signs of structural degradation in sample Z-  $\text{HNO}_3$ . This suggests partial damage to the zeolitic framework due to aggressive acid treatment. In contrast, the sample Z-  $\text{HNO}_3$ -600 (Figure 6c) shows a narrower particle size distribution (7–32  $\mu\text{m}$ ) and a more preserved morphology. The pore openings appear more defined, indicating that thermal treatment can improve pore accessibility without excessive damage to the structure. Finally, the sample Z-MIX-280 (Figure 6d) contains particles range from 7 to 15  $\mu\text{m}$ , which are among the smallest observed across all treatments. A more uniform pore distribution is evident, and the reduced particle size suggests increased surface area and potential applicability in nanoscale catalytic systems. This indicates that the mixed-acid treatment can effectively tailor the surface texture while preserving structural integrity, offering potential advantages for catalytic applications and further exploration as a nanostructured material. In general, the acid treatments promote partial dealumination and modification of the surface texture, while the combined acid-thermal treatment allows for controlled restructuring. These morphological changes are expected to influence the textural properties and catalytic behavior of the zeolite.

Acid treatment of the natural zeolite led to a significant increase in the  $\text{SiO}_2/\text{Al}_2\text{O}_3$  ratio, indicating partial dealumination and enrichment of the siliceous framework (Table 2). A progressive reduction in  $\text{Fe}_2\text{O}_3$ ,  $\text{CaO}$ ,  $\text{Na}_2\text{O}$ , and  $\text{MgO}$  contents after acid washing and thermal treatment suggests efficient removal of exchangeable and loosely bound cations. The sample treated with the mixed acid solution at 280  $^\circ\text{C}$  (Z-MIX-280) exhibited the highest  $\text{SiO}_2$  content (76.04 wt.%) and lowest concentrations of impurities, confirming deeper structural modification and purification. These changes reflect improved acidity and enhanced surface properties favorable for catalytic applications.

**Table 2.** Elemental Composition (wt. %) of Natural and Modified Zeolite Samples Treated with Acids.

Sample	phase composition, mass. %								
	$\text{Al}_2\text{O}_3$	$\text{SiO}_2$	$\text{Fe}_2\text{O}_3$	$\text{MgO}$	$\text{Na}_2\text{O}$	$\text{K}_2\text{O}$	$\text{CaO}$	$\text{TiO}_2$	$\text{H}_2\text{O}$
NZ	15.1	62.2	5.8	3.6	5.8	2.1	4.1	0.7	0.6
Z- $\text{HNO}_3$	16.7	71.4	2.9	2.28	2.6	1.5	2.1	0.02	0.5
Z- $\text{HNO}_3$ -600	18.2	73.5	2.1	1.9	2.2	1.1	1.9	0.01	0.09
Z-MIX-280	20.2	76.04	0.6	0.8	0.7	0.7	0.9	0.01	0.05

The EDAX spectra (Figure 7) illustrate the elemental changes in the zeolite samples before and after acid treatment. The natural zeolite (Figure 7a) contains primarily Si and Al, alongside noticeable amounts of Na, K, Ca, and Mg, reflecting its cation-rich composition. After treatment with nitric acid (Figure 7b), a reduction in these exchangeable cations is observed, accompanied by a slight increase in the Si/Al ratio, indicating initial dealumination. Thermal post-treatment (Figure 7c) further reduces non-framework elements and enhances the silicon content, suggesting improved structural stability. The sample treated with the mixed acid system ( $\text{HNO}_3 + \text{CH}_3\text{COOH}$ , Figure 7d) shows the most pronounced removal of extraneous cations and the highest Si/Al ratio, confirming deeper purification and partial framework reorganization. These EDAX observations correlate well with FTIR and elemental analysis results, confirming selective cation extraction and surface modification while maintaining the zeolite's structural framework.



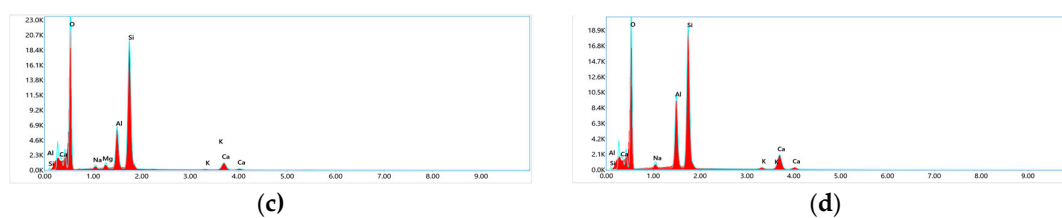


**Figure 7.** Energy-Dispersive X-ray Spectroscopy (EDAX) of the Natural and Modified Zeolite Samples Treated with Acids: (a) – NZ; (b) – Z- HNO<sub>3</sub>; (c) – Z- HNO<sub>3</sub>-600; (d) –Z-MIX-280.

### 3.2. Catalytic Activity of Zeolite

Preliminary tests on thiophene hydrodesulfurization were conducted using both natural and acid-modified clinoptilolite as catalyst supports. The unmodified zeolite exhibited a thiophene conversion of 12,3%, whereas the modified sample (Z-MIX-280) demonstrated an increased conversion of 20,7%, highlighting the positive effect of acid activation on catalytic performance. Although the zeolite itself was used without active metal species, these results indicate its potential as a catalyst support due to enhanced surface area, acidity, and pore accessibility.

The hydrodesulfurization (HDS) of thiophene typically proceeds via hydrogenation of the aromatic ring followed by C–S bond cleavage (Figure 8), producing butane and hydrogen sulfide (H<sub>2</sub>S). While the current study does not include metal species, the improved acidity and porosity of the modified zeolite are expected to facilitate dispersion of active phases and enhance thiophene adsorption and activation in subsequent catalyst formulations.

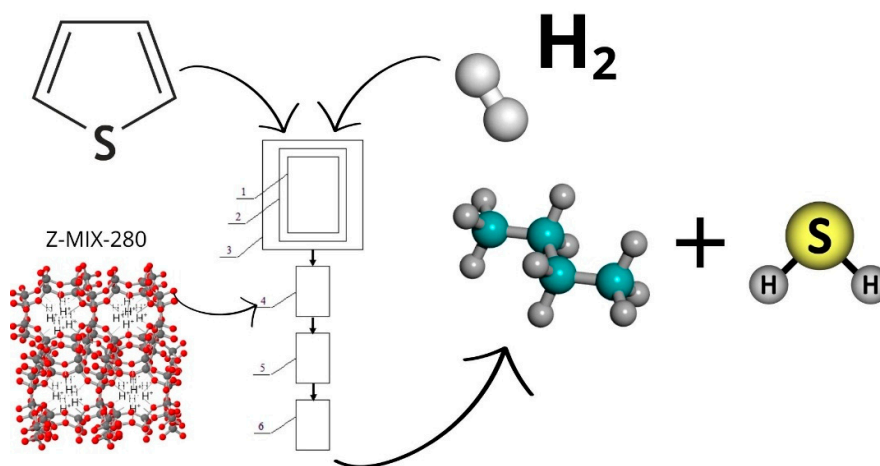


**Figure 8.** Schematic representation of the HDS experimental reactor setup.

Further studies are in progress to synthesize metal-loaded catalysts based on the modified zeolites, aiming to optimize their activity for practical hydrodesulfurization applications.

## 5. Conclusions

This study demonstrates that acid activation significantly enhances the physicochemical properties of natural clinoptilolite from the Shankhanai deposit, making it a viable candidate for catalytic applications. XRD, FTIR, BET, TGA, SEM, and EDX analyses confirmed that 10% nitric acid increases surface area and porosity but partially degrades the framework. In contrast, the combination of 10% nitric acid and 5% acetic acid followed by mild thermal treatment effectively preserved crystallinity while improving microporosity and acidity. This dual-acid method proved to be a more balanced and environmentally friendly strategy for zeolite modification. Preliminary

catalytic tests on thiophene hydrodesulfurization showed increased conversion (from 12.3% to 20.7%) after modification, despite the absence of active metal species. These findings indicate that the modified zeolite can serve as a promising support for further catalyst development aimed at deep desulfurization under mild conditions. Importantly, the study highlights the potential of tailoring acidity and porosity through controlled acid combinations, offering a pathway to design efficient catalyst supports without compromising structural integrity. Future work will focus on the incorporation of active metal species and evaluation of long-term catalytic stability under industrially relevant conditions.

## 6. Patents

**Author Contributions:** S.K. Tanirbergenova and A.N. Aitugan contributed to the conceptualization and design of the study. S.K. Tanirbergenova developed the methodology and software. Validation was performed by S.K. Tanirbergenova, D.A. Tugelbayeva, and N.K. Zhylybayeva. Formal analysis was conducted by S.K. Tanirbergenova and A.N. Aitugan. The investigation was carried out by S.K. Tanirbergenova and D.A. Tugelbayeva. Resources were provided by G.M. Moldazhanova. Data curation was handled by S.K. Tanirbergenova. S.K. Tanirbergenova prepared the original draft of the manuscript, while D.A. Tugelbayeva, N.K. Zhylybayeva, K. Tazhu, and G.M. Moldazhanova contributed to writing—review and editing. Visualization was carried out by A.N. Aitugan. Supervision was provided by S.K. Tanirbergenova and Z.A. Mansurov. Project administration was undertaken by S.K. Tanirbergenova. Funding acquisition was the responsibility of Z.A. Mansurov. All authors have read and agreed to the published version of the manuscript.

**Funding:** This research was funded by the Science Committee of the Ministry of Science and Higher Education of the Republic of Kazakhstan,<sup>1</sup> Grant No. BR24992915

**Data Availability Statement:** We encourage all authors of articles published in MDPI journals to share their research data. In this section, please provide details regarding where data supporting reported results can be found, including links to publicly archived datasets analyzed or generated during the study. Where no new data were created, or where data is unavailable due to privacy or ethical restrictions, a statement is still required. Suggested Data Availability Statements are available in section “MDPI Research Data Policies” at <https://www.mdpi.com/ethics>.

**Acknowledgments:** This research was funded by the Science Committee of the Ministry of Science and Higher Education of the Republic of Kazakhstan,<sup>1</sup> Grant No. BR24992915.

**Conflicts of Interest:** The authors declare no conflicts of interest.

## Abbreviations

The following abbreviations are used in this manuscript:

FTIR	Fourier Transform Infrared Spectroscopy
XRD	X-ray Diffraction
EDAX	Energy Dispersive X-ray Analysis
EDTA	Ethylenediaminetetraacetic Acid
SEM	Scanning Electron Microscopy

## References

1. European Parliament and Council. Directive 2009/30/EC amending Directive 98/70/EC as regards the specification of petrol, diesel and gas-oil and introducing a mechanism to monitor and reduce greenhouse gas emissions; Official Journal of the European Union, 2009.
2. International Maritime Organization (IMO). IMO 2020 – Reducing Sulphur Oxide Emissions.

3. Shafiq, I.; Shafique, S.; Akhter, P.; Alazmi, A.; Naqvi, S.A.R. Recent Developments in Alumina-Supported Hydrodesulfurization Catalysts. *Catal. Rev.* 2020, 62, 96–164. <https://doi.org/10.1080/01614940.2019.1652393>.
4. Wei, W.; Wang, Q.; Wei, X.; Zhang, H.; Zhang, Z.; Ma, X. Tuning Effect of Brønsted Acidity on FeZn Bimetallic HDS Catalyst with Y Zeolite/ $\gamma$ -Al<sub>2</sub>O<sub>3</sub> Support. *Energy Fuels* 2021, 35, 6482–6491. <https://doi.org/10.1021/acs.energyfuels.1c00211>.
5. Al-Otaibi, R.M.; Al-Malki, A.L.; Hossain, M.M. Modification of ZSM-5 Mesoporosity for Enhanced Hydrodesulfurization of DBT. *J. Environ. Chem. Eng.* 2021, 9, 105593. <https://doi.org/10.1016/j.jece.2021.105593>.
6. Jiang, K.; Li, M.; Li, Y.; Jin, Y.; Zhang, J. Adsorption of Sulfur Compounds on AgX Hierarchical Zeolite. *Environ. Sci.: Atmos.* 2021, 1, 377–387. <https://doi.org/10.1039/D1EA00018H>.
7. Wang, Y.; Zhang, T.; Li, L.; Chen, Y. TiO<sub>2</sub> Modified HY Zeolite for Oxidative Desulfurization. *Silicon* 2024, 16, 867–875. <https://doi.org/10.1007/s12633-023-02123-4>.
8. Kim, H.; Lee, D.; Park, J. GO-Modified TiO<sub>2</sub> and Al<sub>2</sub>O<sub>3</sub> Supports for NiMo Hydrodesulfurization Catalysts. *MRS Adv.* 2025, 10, 215–224. <https://doi.org/10.1557/s43580-025-00312-w>.
9. Khrysonidi, V.A.; Kirilenko, V.A.; Khoruzhiy, K.I.; Shatokhina, E.M. Hierarchical zeolites and modern methods of their synthesis. *Sci. Herit.* 2021, 71(1), 10–14.
10. Spiridonov, A.M.; et al. Prospects for the use of acid-activated natural zeolite from the Khonguruu deposit (Yakutia) for filling polymers. *Vestn. Sev.-Vost. Fed. Univ. im. M.K. Ammosova* 2014, 11(3), 7–12.
11. Razmakhnin, K.K.; Khat'kova, A.N. Modification of zeolite properties to expand their application areas. *Gorn. Inf.-Analit. Byul.* 2011, 4, 246–252.
12. Abdulina, S.A.; et al. Features of the mineral composition of zeolite from the Taizhuzgen deposit. *Vestn. Kazakhst. Gos. Tekh. Univ.* 2014, 2, 48.
13. Vasilina, G.K.; Moisa, R.M.; Abildin, T.S.; Yesemaliyeva, A.S.; Kuanysheva, S.D. Influence of the structure of natural zeolites on their acidic characteristics. *Izv. NAN RK. Ser. Khimii i Tekhnologii* 2017, 6, 81–85.
14. Mambetova, M.; Yergaziyeva, G.Y.; Zhoketayeva, A.B. Physicochemical characteristics and carbon dioxide sorption properties of natural zeolites. *Gorenie i Plazmokhimiya* 2022.
15. Akhalbedashvili, L.G. *Catalytic and Ion-Exchange Properties of Modified Zeolites and Superconducting Cuprates*. Ph.D. Thesis, Tbilisi, Georgia, 2006.
16. Koval', L.M.; Korobitsyna, L.L.; Vosmerikov, A.V. *Synthesis, Physicochemical and Catalytic Properties of High-Silica Zeolites*, 3rd ed.; TGU: Tomsk, Russia, 2001; pp. 50.
17. Sultanbaeva, G.Sh.; et al. Physicochemical studies of zeolite activated with hydrochloric acid. *Izv. Nats. Akad. Nauk Resp. Kazakhstan, Ser. Khim.* 2006, 4, 68.
18. Mamedova, G.A. Influence of boiling acids on the structure of natural Nakhchivan mordenite. *Bashk. Khim. Zh.* 2016, 23(3), 20–27.
19. Li, X.; Wang, Y.; Zhang, H.; Chen, J. Modification of natural zeolites for enhanced catalytic activity: A review. *Microporous Mesoporous Mater.* 2023, 347, 112364. <https://doi.org/10.1016/j.micromeso.2022.112364>
20. Chizallet, C.; Bouchy, C.; Larmier, K. Molecular views on mechanisms of Brønsted acid catalyzed reactions in zeolites. *Chem. Rev.* 2023, 123(9), 6107–6196. <https://doi.org/10.1021/acs.chemrev.2c00896>
21. Zhang, Z.; Liu, X.; Yang, M. Acid-modified clinoptilolite for ammonia removal and catalytic applications. *J. Environ. Chem. Eng.* 2021, 9(5), 105927. <https://doi.org/10.1016/j.jece.2021.105927>
22. Shah, M.T.; et al. Acid-modified zeolite for removal of environmental pollutants: Mechanism and efficiency. *Environ. Sci. Pollut. Res.* 2020, 27(3), 3155–3170. <https://doi.org/10.1007/s11356-019-07094-3>
23. Celik, G.; Patel, A.; Choudhary, V. Tailoring the surface acidity of clinoptilolite for catalytic applications: A comparative study of HCl and NH<sub>4</sub>Cl treatments. *Microporous Mesoporous Mater.* 2022, 342, 111591. <https://doi.org/10.1016/j.micromeso.2022.111591>
24. Teshima, K.; Kinoshita, K.; Tanaka, K. Structural evolution of clinoptilolite upon acid treatment. *Appl. Clay Sci.* 2020, 184, 105402. <https://doi.org/10.1016/j.clay.2019.105402>
25. Miądlicki, P.; Wróblewska, A.; Kiełbasa, K.; Koren, Z.C.; Michalkiewicz, B. Sulfuric acid modified clinoptilolite as a solid green catalyst for solvent-free  $\alpha$ -pinene isomerization process. *Microporous Mesoporous Mater.* 2021, 324, 111266. <https://doi.org/10.1016/j.micromeso.2021.111266>

26. Tanirbergenova, S.; Tagayeva, A.; Rossi, C.O.; Porto, M.; Caputo, P.; Kanzharkan, E.; Tugelbayeva, D.; Zhylybayeva, N.; Tazhu, K.; Tileuberdi, Y. Studying the Characteristics of Tank Oil Sludge. *Processes* **2024**, *12*(9), 2007. <https://doi.org/10.3390/pr12092007>
27. Sadenova, M.A.; Abdulina, S.A.; Tungatarova, S.A.; et al. The use of natural Kazakhstan zeolites for the development of gas purification catalysts. *Clean Technol. Environ. Policy* **2016**, *18*(2), 449–459. <https://doi.org/10.1007/s10098-015-1018-6>
28. Jiang, N.; Shang, X.; Zhang, T.; Liu, X.; Zhang, Q.; Liu, H.; Lu, X. Study on the Pyrolysis Characteristics and Kinetics of Lignite Blended with Biomass. *Molecules* **2020**, *25*(11), 2570. <https://www.mdpi.com/1420-3049/25/11/2570>
29. Aitugan, A.N.; Tanirbergenova, S.K.; Tileuberdi, Ye.; Yucel, O.; Tugelbayeva, D.; Mansurov, Z.; Ongarbayev, Ye.K. A carbonised cobalt catalyst supported by acid-activated clay for the selective hydrogenation of acetylene. *React. Kinet. Mech. Catal.* **2021**, *133*(1), 277–292.
30. Khalid, M.; et al. Natural zeolites in water treatment: Potentials and limitations. *Chemosphere* **2020**, *245*, 125624. <https://doi.org/10.1016/j.chemosphere.2019.125624>
31. Zahid, M.; Doszhanov, Y.; Saurykova, K.; et al. Modification and Application of Natural Clinoptilolite and Mordenite from Almaty Region for Drinking Water Purification. *Molecules* **2025**, *30*(9), 2021. <https://doi.org/10.3390/molecules30092021>
32. Velichkina, L.; Barbashin, Yu.; Vosmerikov, A. Effect of Acid Treatment on the Properties of Zeolite Catalyst for Straight-Run Gasoline Upgrading. *Catal. Res.* **2021**, *1*(4), 16. <https://www.lidsen.com/journals/cr/cr-01-04-016>
33. Tsitsishvili, V.; et al. Acid treatment of Georgian, Kazakhstani and Armenian natural heulandite-clinoptilolites II. Adsorption and porous structure. *InterConf.* **2023**, March. <https://doi.org/10.51582/interconf.19-20.03.2023.052>

**Disclaimer/Publisher's Note:** The statements, opinions and data contained in all publications are solely those of the individual author(s) and contributor(s) and not of MDPI and/or the editor(s). MDPI and/or the editor(s) disclaim responsibility for any injury to people or property resulting from any ideas, methods, instructions or products referred to in the content.